

PAHs contents in road dusts on principal roads collected nationwide in Japan and their influential factors

Noriatsu OZAKI¹, Yuma AKAGI², Tomonori KINDAICHI¹, Akiyoshi OHASHI¹

¹ Graduate school of Engineering, Hiroshima University, Higashihiroshima, 1-4-1, Higashihiroshima, 739-8527, Japan

(E-mail: ojaki@hiroshima-u.ac.jp)

² Hiroshima University, Higashihiroshima, 1-4-1, Higashihiroshima, 739-8527, Japan

(Present: Okayama Prefectural Bureau)

Abstract

54 Road dust samples were collected in principal roads ($n=37$) and residential roads ($n=17$) nationwide in Japan from March 2010 to November 2012. Sixteen polycyclic aromatic hydrocarbons (PAHs) and ignition loss (IL) were determined. The total PAHs contents ranged from 62 to 6,325 ng g⁻¹ with a geometric mean of 484 ng g⁻¹. The IL ranged from 0.8-17% with a mean of 6%. The PAHs contents were correlated with the IL contents, and the IL contents were dependent on the population density. From the PAHs patterns analysis, the PAHs of road dust is considered to be majorly from the diesel emissions.

Keywords

Polycyclic aromatic hydrocarbons; PAHs; road dust; principal road; traffic density

INTRODUCTION

Increased runoff of toxic substances from urban areas has become a serious problem. There are many types of toxic substances that enter urban runoff, including metals, pharmaceuticals, personal care products and unintentionally created organic substances. One important class of pollutants are polycyclic aromatic hydrocarbons (PAHs). PAHs are a group of organic compounds composed of two or more fused benzene rings, many of which have been shown to be carcinogenic and mutagenic (Dipple 1985; Vinggaard et al., 2000; Xue et al., 2005). PAHs primarily originate from the incomplete combustion of fossil fuels, which results in their emission into the atmosphere and subsequent deposition into aquatic environments. In our previous studies (Ozaki et al, 2012; Kojima et al, 2010; Iwasaki et al, 2009), PAHs were extensively investigated in the Hiroshima Bay area, Japan. The results showed that considerable differences were apparent between atmospheric and sediment PAH loadings in the bay. The estimated atmospheric deposition of PAHs was considerably lower than the deposition estimated for sediments in the bay. To understand this difference it is important to investigate the behavior of road dust because road dust deposition is an important pathway for pollutants from air to enter water (Rogge et al, 1992; Aryal et al, 2005, 2013; Murakami et al, 2005; Liu et al, 2007; Hassanien and Abdel-Latif, 2008; Zhang et al 2008). For example, if PAH concentration patterns in road dust are different from those measured in the atmosphere, the PAHs in road dust would then be assumed to have originated from different sources than just the atmosphere. Some mechanically-generated dust particles deposit more readily by gravitational sedimentation and are not easily re-suspended in the atmosphere (Rogge et al, 1992). It is difficult to measure this pathway using typical bucket sampling for atmospheric deposition, so direct sampling of road dust may provide a way to better understand this potential pathway. In this study, road dust on major and residential roads across Japan was collected and PAH concentrations were measured. From the results, PAH concentration patterns were compared with those from vehicle emissions and atmospheric particles.

MATERIALS AND METHODS

Samplings

The road dusts were collected nationwide in Japan, and 54 samples were collected from Hokkaido, the north most prefecture, to Okinawa, the south most in Japan, from March 2010 to November

2012 (**Table 1**). The number of principal road sampling was 37, and the 17 samples were obtained on residential roads. The samples were collected during the daytime (10:30–19:00), and in order to avoid direct effects of rainfall, a sample was collected in a dry day after more than two days from the antecedent rainfall (two samples were less than 48 hours). The samples were collected at the edge of the roads using a brush of swine bristles. The pavement of the roads was asphalt in all. The area of the samples were 0.18–5.15 m² and the resultant collected particle mass was 10–200 g per sample. Traffic density data was obtained from the road traffic census by Ministry of Land, Infrastructure, Transport and Tourism of Japan (the latest census was 2010). The traffic density of the sampled principal road ranged from 4,507–67,935 vehicles d⁻¹. The climate data was obtained from from the AMeDAS data set supplied by the Japan Meteorological Agency.

Table 1. Sampling Points with measured 16PAHs and IL

ID	Sampling date	GPS coordinate (WGS84)	Location (City)	Route	Principal road? [Y/N]	Traffic dens. [Vehicles d ⁻¹]	Weather cond.	Temp. [°C]	Antecedent rainfall [mm]	Antecedent dry period [hr]	16PAHs [ng g ⁻¹]	IL [-]
100329-34-01	2010/03/29 15:00	34.393886,132.456894	Hiroshima	NR route 54	Y	36,228	Fine	11.5	16.5	100	142	0.018
100506-13-01	2010/05/06 15:00	35.707593, 139.766967	Tokyo	PR Route 453	Y	21,207	Fine	24.4	83.5	168	388	0.108
100517-13-02	2010/05/17 10:30	35.650348, 139.753609	Tokyo	NR Route 15	Y	45,109	Fine	23.2	16.5	123	1653	0.135
100517-13-03	2010/05/17 12:00	35.64351, 139.810503	Tokyo	TM highway	Y	46,280	Fine	24.4	16.5	124	1340	0.100
100517-13-04	2010/05/17 14:00	35.690699, 139.798037	Tokyo	TM Route 483	Y	24,113	Fine	25.5	16.5	126	365	0.070
100520-43-01	2011/05/20 12:00	32.814272,130.726407	Kumamoto	Kumamoto PR Route 337	Y	18,392	Fine	28.3	6.5	217	139	0.074
100806-09-01	2010/08/06 00:00	36.343941, 139.459554	Ashikaga		N	-	Fine	-	8.5	77.0	188	-
100806-09-02	2010/08/06 00:00	36.343941, 139.459554	Ashikaga		N	-	Fine	-	8.5	78.0	1802	-
100806-09-03	2010/08/06 00:00	36.315319, 139.492282	Ashikaga		N	-	Fine	-	8.5	79.0	121	-
100823-27-01	2010/08/23 10:35	34.842100, 135.567308	Osaka	Osaka PR Route 46	Y	17,974	Fine	36.2	17.0	222	690	0.041
100903-25-01	2011/09/03 14:00	35.047416, 135.918055	Kusatsu	Shiga PR Route 559	N	-	Fine	36.0	7.0	116	1093	0.073
100903-26-01	2011/09/03 15:40	34.995972, 135.742611	Kyoto	NR Route 9	Y	57,356	Fine	35.0	135.5	531	6325	0.173
100903-26-02	2011/09/03 14:15	34.991722, 135.752805	Kyoto	NR Route 1	Y	43,186	Fine	35.5	135.5	530	3204	0.141
100911-01-01	2010/09/11 08:30	43.342032, 142.360867	Furano		N	-	Fine	19.3	30.0	119	625	0.041
101028-01-01	2010/10/28 23:00	42.633959,141.602955	Tomakomai	NR Route 36	Y	27,795	Cloudy	1.9	21.0	44	417	0.008
101116-43-01	2010/11/16 06:00	32.797331, 130.704788	Kumamoto		N	-	Fine	4.4	7.5	97	373	0.063
110105-34-01	2011/01/05 10:00	34.489615,133.39797	Fukuyama	NR Route 1	Y	44,115	Cloudy	3.5	15.5	349	494	
110105-34-02	2011/01/05 10:00	34.507927,133.410158	Fukuyama	Hiroshima PR Route 379	Y	17,585	Cloudy	3.5	15.5	349	336	0.034
110105-34-03	2011/01/05 10:00	34.516211,133.440714	Fukuyama		N	-	Cloudy	3.5	15.5	349	184	-
110120-34-04	2011/01/20 20:00	34.403156,132.752094	Higashihiroshima	NR Route 2	Y	25,598	Fine	0.6	3.5	404	691	0.055
110120-34-05	2011/01/20 20:00	34.421673,132.75291	Higashihiroshima	NR Route 375	Y	15,582	Fine	0.6	3.5	404	282	0.055
110120-34-06	2011/01/20 20:00	34.414628,132.742653	Higashihiroshima		N	-	Fine	0.6	3.5	404	238	0.025
110128-24-01	2011/01/28 12:20	34.767305, 136.130583	Iga		N	-	Cloudy	6.0	5.5	668	297	0.029
110128-27-01	2010/01/28 16:50	34.842100, 135.567308	Ibaragi	Osaka PR Route	Y	17,974	Fine	6.5	11.0	906	705	0.047
110128-27-02	2011/01/28 09:25	34.789416, 135.57975	Ibaragi	Osaka PR Route	Y	4,507	Fine	6.5	11.0	899	1510	0.034
110128-28-01	2011/01/28 15:30	34.90625, 135.409777	Kawanishi	Hyogo PR Route	Y	-	Fine	4.5	13.0	905	701	0.072
110128-29-01	2011/01/28 10:50	34.692527, 135.811638	Nara	NR Route 24	Y	49,189	Fine	7.5	6.0	685	332	0.056
110226-34-01	2011/02/26 17:00	34.414891,132.454082	Hiroshima	NR Route 183	Y	22,395	Fine	12.2	18.0	209	322	0.017
110414-34-01	2011/04/14 12:00	34.433437,132.791719	Higashihiroshima	Sanyo highway	Y	41,697	Fine	18.2	20.5	135	436	0.056
110518-23-01	2011/05/18 19:00	35.170991,136.889542	Nagoya	Aichi PR Route 63	N	-	Fine	22.6	3.5	148	1775	0.122
110521-33-01	2011/05/21 13:00	34.68161,133.914365	Okayama	NR Route 53	Y	41,548	Fine	25.6	14.0	217	463	0.023
110619-34-01	2011/06/19 18:00	34.57526,133.237542	Fuchu	Hiroshima PR Route 218	N	-	Cloudy	23.3	6.5	65	378	0.019
110801-34-01	2011/08/01 19:00	34.411383,133.203046	Onomichi	NR Route 2	Y	15,096	Fine	29.4	13.0	323	740	0.024
111125-23-01	2011/11/25 11:30	35.09291,136.92489	Nagoya	Aichi PR Route 55	Y	30,150	Cloudy	11.0	59.0	138	2768	0.165
111202-34-01	2011/12/02 11:00	34.443745,132.653	Higashihiroshima	NR Route 2	Y	24,034	Fine	10.0	58.0	308	610	0.041
111205-12-01	2011/12/05 23:00	35.723388,140.075136	Yachiyo	NR Route 296	Y	29,984	Fine	6.5	28.0	58	620	0.054
111215-34-02	2011/12/15 15:30	34.390842,132.719082	Higashihiroshima	Hiroshima PR Route 331	Y	11,193	Fine	8.5	5.0	173	291	0.016
111215-34-03	2011/12/15 16:00	34.433437,132.791719	Higashihiroshima	Sanyo highway	Y	41,697	Fine	8.1	5.0	173	1046	0.064
111215-34-06	2011/12/15 17:00	34.428764,132.848659	Takehara	Hiroshima PR Route 351	N	-	Fine	7.8	5.0	174	706	0.056
120106-13-01	2012/01/06 14:00	35.679793,139.77183	Tokyo	NR Route 15	Y	19,155	Fine	9.6	4.0	651	2815	0.158
120421-34-01	2012/04/21 18:00	34.667322,132.705226	Akitakata	Hiroshima PR Route 54	Y	16,910	Fine	17.0	45.0	245	181	0.020
120809-32-01	2012/08/09 17:00	35.434163,133.012011	Matsue	NR Route 9	Y	37,823	Fine	26.2	10.5	617	474	0.021
120809-32-02	2012/08/09 18:00	35.319509,132.912061	Utsunomiya	NR Route 54	Y	10,422	Fine	24.3	21.0	618	391	0.051
120826-34-01	2012/08/26 19:00	34.39,132.9347	Mihara	NR Route 2	Y	18,874	Fine	27.8	33.5	298	490	0.024
120904-23-01	2012/09/04 18:30	35.16934,136.911541	Nagoya	Aichi PR Route 60	N	-	Cloudy	27.5	26.0	413	297	0.059
120905-23-01	2012/09/05 19:30	35.171486,136.919585	Nagoya	NR Route 153	Y	40,741	Fine	28.8	26.0	438	138	0.042
120906-23-01	2012/09/06 20:30	35.170594,136.897443	Nagoya	NR Route 19	Y	67,935	Cloudy	28.3	26.0	443	89	0.029
120910-41-01	2012/09/10 11:00	33.260291,130.298632	Saga	Saga PR Route 29	N	-	Cloudy	25.3	16.0	123	157	0.030
120911-41-01	2012/09/11 15:30	33.250101,130.294955	Saga	NR Route 264	Y	22,180	Fine	25.8	16.0	136	512	0.026
120917-47-01	2012/09/17 20:30	26.245176,127.694631	Urasoe	NR Route 58	Y	67,013	Fine	27.0	135.5	32	232	0.049
120919-47-01	2012/09/19 11:30	26.239419,127.705537	Urasoe	Okinawa PR Route 251	N	-	Cloudy	25.8	135.5	72	226	0.049
120922-47-01	2012/09/22 12:00	26.236494,127.697412	Naha	Okinawa PR Route 82	N	-	Cloudy	27.7	135.5	140	62	0.021
121020-34-01	2012/10/20 18:00	34.397167,133.0895	Mihara	NR Route 2	Y	29,359	Fine	16.9	37.0	71	826	0.049
121110-13-01	2012/11/10 08:30	35.727634,139.768581	Tokyo		N	-	Fine	13.6	41.0	87	927	0.106

NR: national route, PR: prefectural route TM: Tokyo metropolitan

The samples were dried in a desiccator at room temperature in 48 hours in dark and sieved and

particles with <2 mm were obtained. The samples were stored in -4 °C prior to the measurements. Laboratory glasswares for analytical purposes were cleaned using dichloromethane (DCM) and glass fibers were burned in 400°C in one hour preliminary. The ignition loss (IL; 600°C, 4 hours) was measured for the samples (four samples were failed to measure). For PAHs extraction, a sample was extracted with DCM in an ultrasonic water bath and the extract was concentrated into 2 mL by N₂-gas. For internal standards, the mixture of acenaphthene-d10, phenanthrene-d10, chrysene-d12, perylene-d12 was applied. The mixed standard was added in vials for instrumental analysis to correct GC/MS-peak detection sensitivity for instrumental analysis.

Instrumental analysis

The PAH concentration was analyzed by using a gas chromatograph equipped with a mass spectrometer (GC-17A/MS-QP5050; SHIMADZU) and operated in the single-ion monitoring mode. Injection was split with the detector, and the inlet temperature was set at 280°C. The initial temperature was 80°C held for 2 min, ramped at 30°C min⁻¹ to 210°C, ramped at 5°C min⁻¹ to 295°C, and ramped at 2°C min⁻¹ to 315°C with 16 mL min⁻¹ He as carrier gas. The mass transfer line and ion source were held at 250°C. Sixteen unsubstituted PAHs were measured (Table 2).

Table 2. List of measured PAHs and their instrumental detection limits

Name	Abbreviation	IDL* (pg)	Name	Abbreviation	IDL* (pg)
Acenaphthylene	Acty	0.10	Chrysene	Chr	0.10
Acenaphthene	Acen	0.10	Benzo(b)fluoranthene	B(b)F	0.14
Fluorene	Flu	0.23	Benzo(k)fluoranthene	B(k)F	0.45
Phenanthrene	Phe	0.10	Benzo(e)pyrene	B(e)P	0.10
Anthracene	Ant	0.10	Benzo(a)pyrene	B(a)P	0.50
Fluoranthene	Flt	0.10	Dibenzo(ah)anthracene	D(ah)A	0.74
Pyrene	Pyr	0.10	Benzo(ghi)perylene	B(ghi)P	0.38
Benzo(a)anthracene	B(a)A	0.10	Indeno(123-cd)pyrene	Ind	0.43

*IDL: Instrument detection limit (pg injected)

Quality control

The detection limit was set at the level of 3 in the SN ratio. Instrument detection limits (IDL) ranged from 0.1–1 pg for each species. Within this level, the coefficient of variation of each of the compounds was less than 20%. The quality of extraction was checked using dried marine sediments (HS-3B, National Research Council of Canada Institute for Marine Biosciences), and the diesel particulate matter (NIST SRM2975). The recovery averaged 50–80% for the marine sediments and 40–60% for the diesel particulate matter for all PAHs, and the repetition error was 5–10%.

RESULTS AND DISCUSSIONS

Fixed-point observation

In order to know the variability of each sampling, the variation of different measurements at a fixed sampling point were checked. For this purpose, the road dusts were collected at a principal road in the vicinity of the laboratory. The point was on Saijo-bypass of the national route 2 (N34.419 E132.722, WGS84). The traffic density was 25,598 vehicles d⁻¹. At the site, samples were taken from three different points (point A, B, and C) on the edge of the road. The distance between A and B, and B and C were 80 and 90m, respectively. The sample was taken six times from 2012/10/15–11/02 during daytime (12:00–18:00). Rainfall occurred twice between the second and third samplings, and the fifth and sixth samplings. **Figure 1** shows the results of the sum of sixteen PAHs (16PAHs) and from the results, the contents (ngPAHs ng⁻¹soil) values were fairly stable for the each of the simultaneous samplings of the different sampling points. In the samplings in '13/10/19 (4th sampling), all the three samples were as twice high as others commonly. This means PAHs contents can vary twofold, and at the same time, spatial variation is less in the order of one hundred meter along the road.

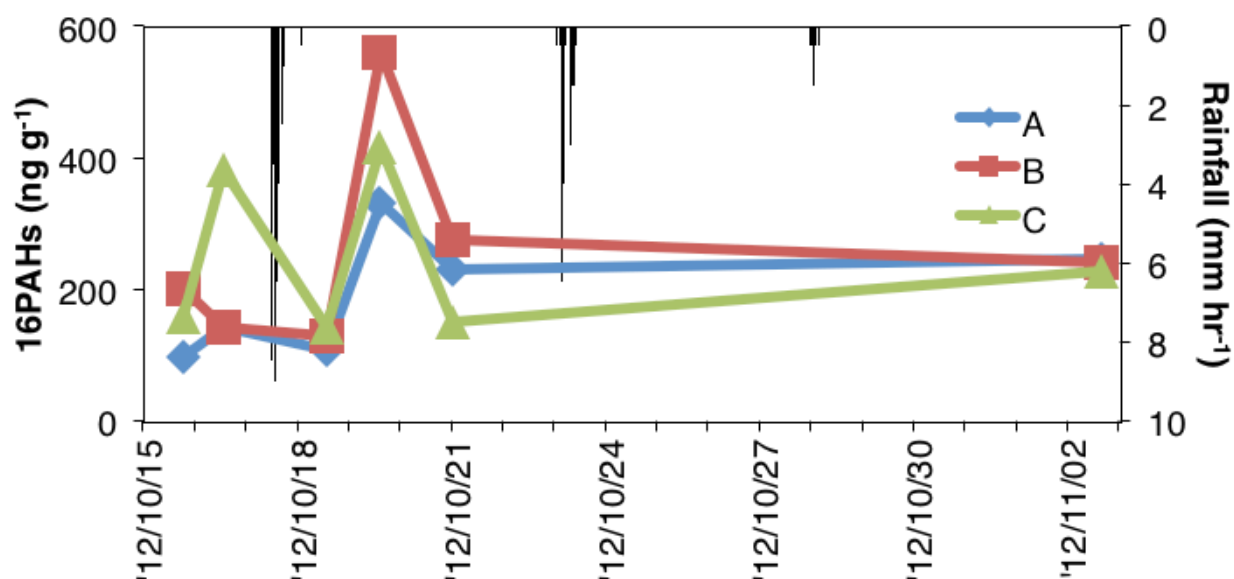


Fig. 1. 16PAHs contents of fixed-point observation

Road samplings

The sixteen PAHs contents varied in two orders ($62\text{--}6,325\text{ ng g}^{-1}$) with the geometric mean of 484 ng g^{-1} ($n=54$) (Table 1). The ILs, organic contents, were $0.8\text{--}17\%$ (mean: 6%). The 16PAHs of the principal loads was 525 ng g^{-1} (geometric mean, $n=37$). The 16PAHs contents patterns were shown in Fig. 2 and the major PAHs species found were fluorene, phenanthrene, fluoranthene, pyrene, and benzo(ghi)perylene.

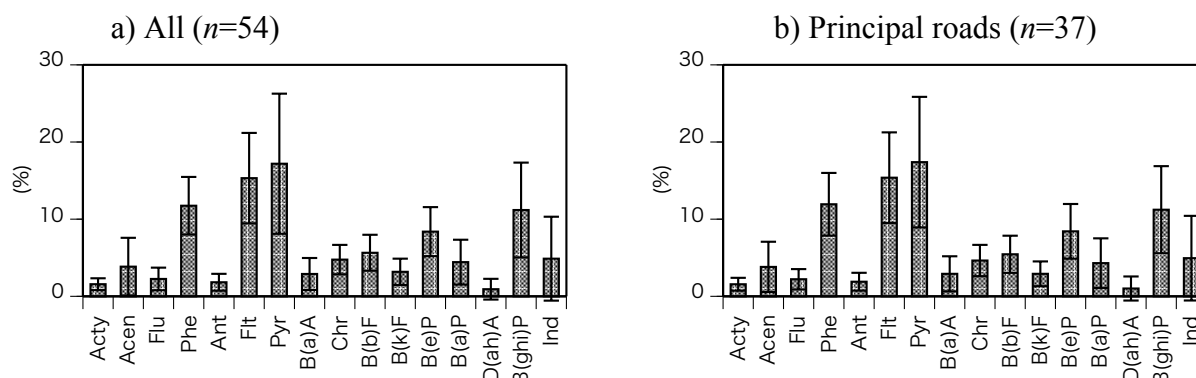


Fig. 2. PAH contents pattern of road dust (error bars represent standard deviation)

Correlations among the 16 PAHs, IL, traffic density, air temperature and population density

The correlation between the contents of all 16 PAHs and IL is shown in Fig. 3. IL, which represents the organic matter present, was well correlated with PAH contents, suggesting that IL and PAHs had the same source or sources. A similar observation was made for road runoff samples (Aryal et al, 2015). The slope value ($2.0 \times 10^4\text{ ng 16 PAHs g}^{-1}\text{ IL}$) indicates that the average PAH contribution to total organic matter was defined by IL. Taking a closer look at the correlation, the 16 PAHs contents seem to increase from the IL of more than 10% , and not simply follow a linear relationship. From this observation, PAH contents divided by organic matter ($\text{ng 16 PAHs g}^{-1}\text{ IL}$) is considered to be another better index for the pollution status. No significant correlation was, however, observed with socioeconomic indices such as traffic or population density. Further research is needed for this.

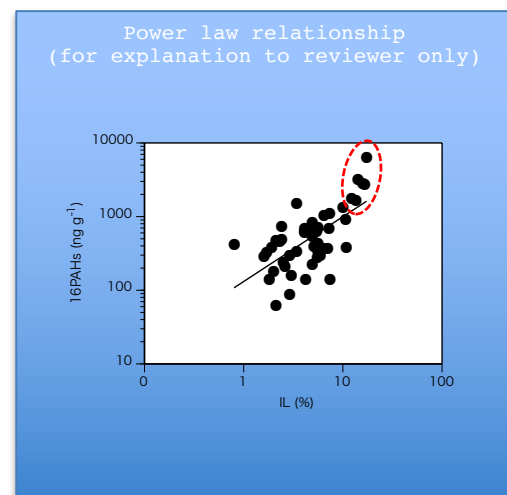
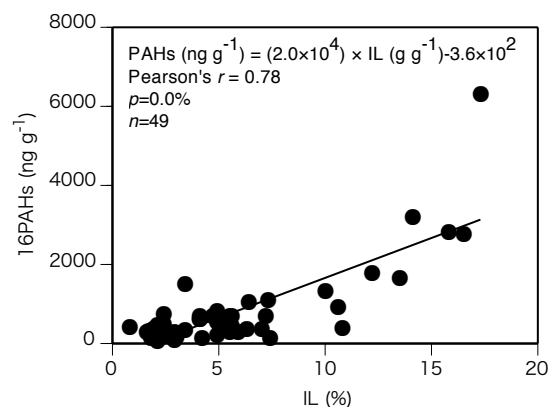


Fig. 3. IL vs. 16PAHs contents

The correlations between 16 PAH contents and traffic density, 16 PAH contents and air temperature, and 16 PAH contents and antecedent rainfall for principal roads are shown in **Fig. 4**. No significant correlations were apparent. Data shown in **Fig. 4** appears to include some outliers. As such, a Spearman's correlation t -test should be preferred instead of a Pearson's t -test. From the t -test, no significant correlation was measured. Traffic activity and population density (average for 10×10 km²; the data were acquired from the National Land Numerical Information download service provided by the Japanese Ministry of Land and Infrastructure) could also have a strong influence on PAH contents, but no significant correlation was identified. Instead of using the PAH contents, the IL contents were found to be correlated with population density (**Fig. 5**). This suggests that these indices were a better estimator of the road dust pollution. IL is easier to measure than PAHs and the population density likely reflects average vehicle activities better than measures like traffic density obtained at a measured site.

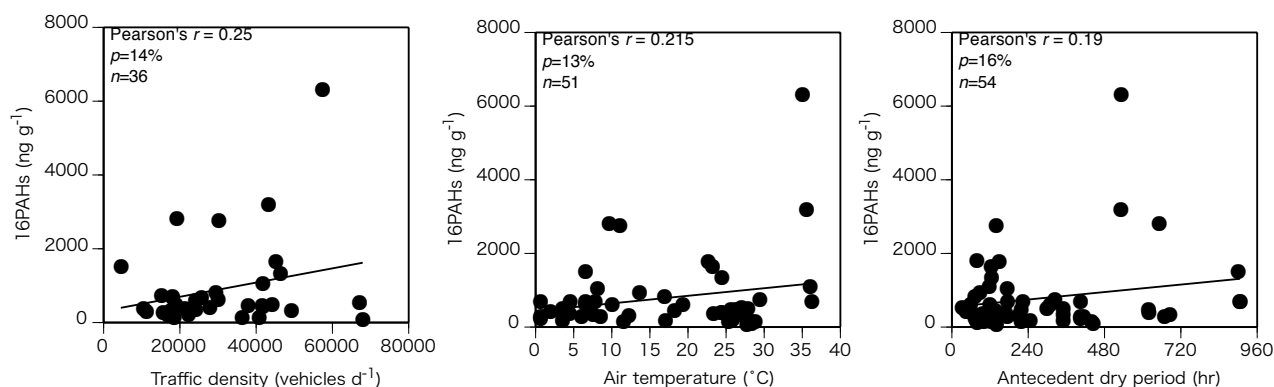


Fig. 4. Traffic density, air temperature, and antecedent dry period vs. 16PAHs contents

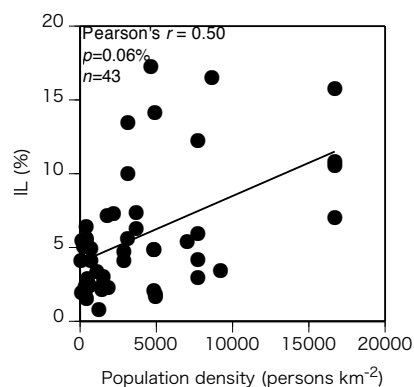
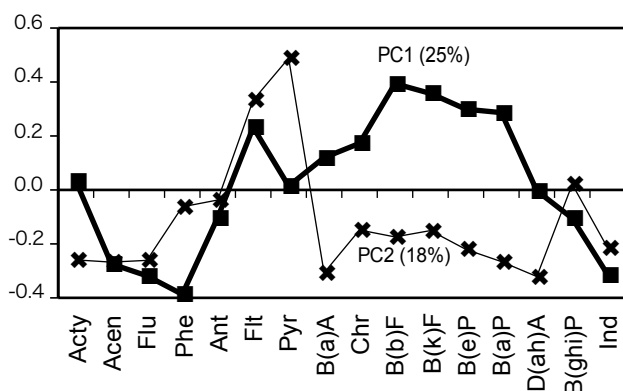


Fig. 5. Population density vs. IL

PAHs pattern analysis

Principal components analysis (PCA) and cluster analysis were conducted for the PAH contents pattern normalized to the sum of the 16 PAHs. Two principal components (PC1 (25%) and PC2 (18%)) were identified (**Fig. 6a**). Also, plots of the two principal component scores are presented with the classifications of the plots by cluster analysis where they were classified into two groups. They were also classified into two separate groups by the population density (**Fig. 6b**). Population density was segmented as being greater than or less than 2,000 people per square kilometer, which was similar to the median value of all the sampling points (1,828 per square kilometer). The PCA or cluster analysis classification did not simply correspond with socioeconomic factors like the population density. In the plots for low population density, the data was more widely scattered than that for high population density for the PC1 score ($p = 0.7\%$ from the F-test). This suggests that there were many emission sources in an urban area and the total load is an averaged mixture of a number of sources in higher population density areas, and in lower population density areas, on the contrary, the number of emission sources would be limited and this possibly caused the PAH pattern observed. More research would be required to confirm this suggestion.

a) PC1 and PC2 patterns



b) PC1 and PC2 scores with cluster analysis grouping (Gr1 and Gr2)

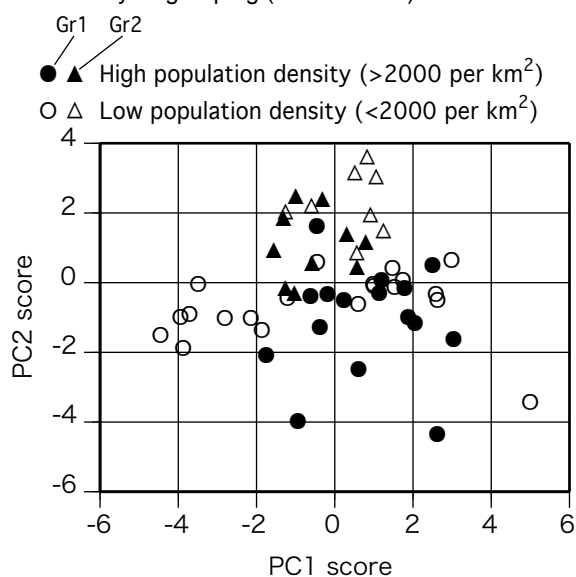


Fig. 6. PCA and cluster analysis results

Isomer ratio analysis of parent PAHs has been widely applied to identify their emission sources (Feng et al, 2006; Yunker et al, 2002). In this study, five widely applied isomer ratios were

calculated (**Fig. 7**). The results are shown with those from other emission sources and under different environmental conditions (vehicle emissions, biomass burning residues, atmospheric particles in cold season and atmospheric deposition) measured and collected in our previous studies (Ozaki et al, 2006, 2012, Fukushima et al, 2012). These results show that Ant/(Ant+Phe) was 0.1–0.2, Flt/(Flt+Pyr) was 0.4–0.6, B(a)A/(B(a)A+Chr) was 0.2–0.5, B(a)P/(B(a)P+B(e)P) was 0.2–0.5 and Ind/(Ind+B(ghi)P) was 0.1–0.6. In comparison to the different emission sources it was difficult to identify just one source.

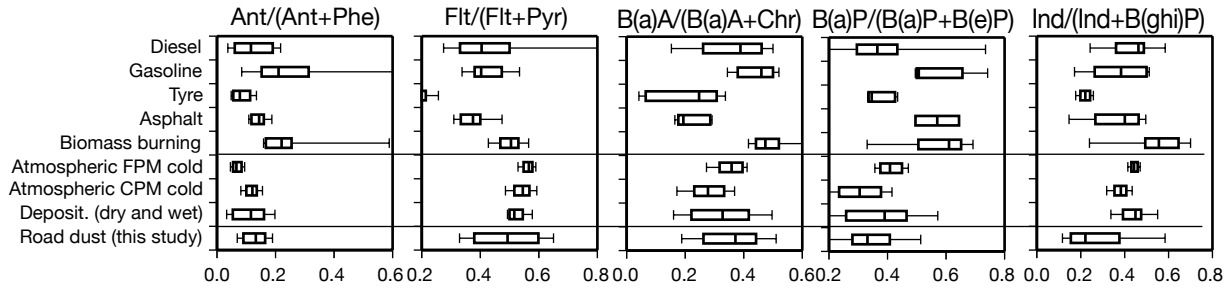


Fig. 7. Isomer ratio analysis (Box and whisker plot; FPM: fine particulate matter (<7 μ m); CPM: coarse particulate matter (>7 μ m); Deposit.: atmospheric deposition)

Using the data sets above, the value of the ratio was statistically compared for each ratio and each emission source using an unpaired t -test with Cohen's d as follows (Cohen 1988):

$$d = \frac{|\bar{x}_1 - \bar{x}_2|}{s},$$

$$s = \sqrt{\frac{(n_1 - 1)s_1^2 + (n_2 - 1)s_2^2}{n_1 + n_2 - 2}},$$

where the subscript 1 and 2 indicate different environmental sources or conditions, \bar{x}_1 and \bar{x}_2 are the mean values, n_1 and n_2 are the data numbers, and the s_1 and s_2 are the standard deviations.

As the d value increases, the difference between the two datasets increases (Thalheimer and Cook 2002, 2008). Using the criteria of Thalheimer and Cook (2002, 2008), differences in the datasets for road dust and other sources were compared for each isomer ratio (**Table 3**). In **Table 3**, the darker colors indicate greater similarities. Diesel was identified to be the most similar to road dust.

Table 3. Comparison of the different emission sources to the road dusts for each isomer ratios by Cohen's d .

	Ant/(Ant+Phe)	Flt/(Flt+Pyr)	B(a)A/(B(a)A+Chr)	B(a)P/(B(a)P+B(e)P)	Ind/(Ind+B(ghi)P)
Diesel	0.24	0.45	0.17	0.64	0.71
Gasoline	1.40	0.49	0.76	1.84	0.51
Tyre	0.68	2.36	1.32	0.24	0.35
Asphalt	0.20	0.88	1.21	1.68	0.40
Biomass burning	1.24	0.10	1.15	1.54	1.34

Finally, to consider the variability of the ratios within the road dust dataset, every ratio was compared to that measured in the surrounding environment. For the comparison, each ratio was

compared to the population density (**Fig. 8**) because the population density was the only parameter for which a significant correlation was identified (**Fig. 5**). No significant correlation was found (*t*-test with Bonferroni correction). But when two outliers were excluded, significant correlations were identified for Ant/(Ant+Phe) and B(a)A/(B(a)A+Chr). One possible explanation for this observation is the sample freshness. Anthracene and benzo(a)anthracene are less stable than their isomers phenanthrene and chrysene, respectively (Yunker and MacDonald, 1995). Therefore, the Ant/(Ant+Phe) and B(a)A/(B(a)A+Chr) ratios could decrease in samples with longer residence times on the roadside. The residence time of ground surface dust would be longer in rural areas and this difference could affect the ratio. These two ratios could provide an indication of PAH residence times on the ground.

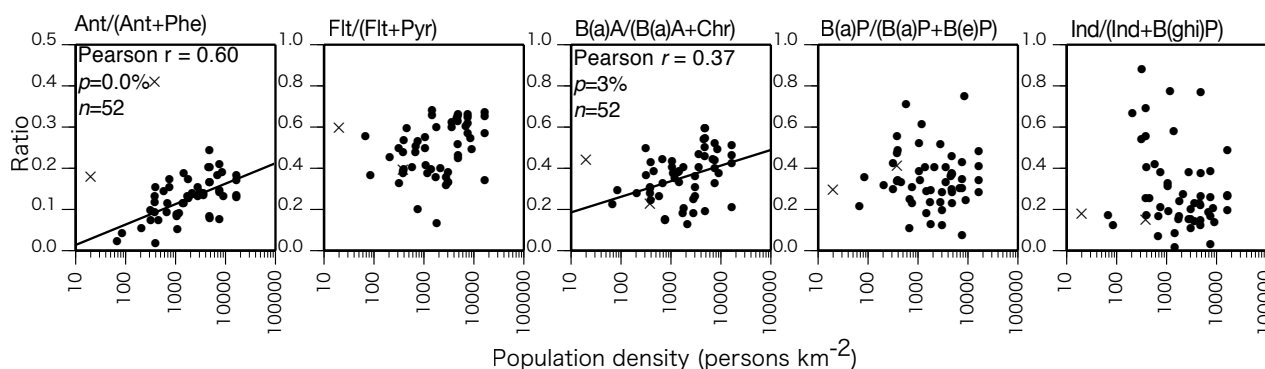


Fig. 8. Population density and Isomer ratios

(The correlation results for Ant/(Ant+Phe) and B(a)A/(B(a)A+Chr) were obtained after the two data points were excluded as outlier (cross marks))

CONCLUSIONS

PAH concentrations and patterns were identified for road dust samples collected from principal roads throughout Japan. PAH contents were correlated with the contents of organic matter; and the organic matter contents were dependent on the population density. Though the PAH contents fluctuated, the ignition loss content is suggested to be a possible index of PAH pollution in road dust. From the PAH pattern analysis, road dust PAHs in Japan were similar in composition to those produced from diesel emissions. For future studies, the combination of total organic matter and PAH pattern analysis would be a promising technique for clarifying the deposition mechanism of urban non-point source pollution. It would also be important to compare road dust composition with atmospheric and water samples using this technique.

ACKNOWLEDGEMENTS

I would like to offer my special thanks to Dr. Keiko WADA, Dr. Michio MURAKAMI, Dr. Hidetoshi KUMATA for the collaboration of the sampling campaign.

REFERENCES

- Aryal R.K., Furumai H., Nakajima F. and Boller M. (2005) Dynamic behavior of fractional suspended solids and particle-bound polycyclic aromatic hydrocarbons in highway runoff, *Water Research*, 39(20), 5126–5134.
- Aryal R., Furumai H., Nakajima F. and Beecham S. (2013) Variation in PAH patterns in road runoff, *Water Science and Technology*, 67(12), 2699–2705.
- Aryal R., Furumai H., Nakajima F., Beecham S. and Lee, B.K. (2015) Analysis of the built-up processes for volatile organics and heavy metals in suspended solids from road run-off,

Desalination and Water Treatment, 54, 1254–1259.

Cohen J. (1988). *Statistical power analysis for the behavioral sciences* (2nd ed.). Hillsdale, NJ: Lawrence Erlbaum.

Dipple A., (1985) Polycyclic aromatic hydrocarbon carcinogenesis, *ACS. Symp. Ser. (Am.Chem.Soc)*, 283–285.

Feng, J.L., Hu, M., Chan, C.K., Lau, P.S., Fang, M., He, L.Y. and Tang, X.Y. (2006) A comparative study of the organic matter in PM_{2.5} from three Chinese megacities in three different climatic zones. *Atmospheric Environment* 40 (21), 3983–3994.

Fukushima T., Watanabe K., Kamiya K. and Ozaki N. (2012) Vertical distributions of PAHs in the sediments of four lakes in Japan, *J. Soils and Sediments*, 12(10), 1530–1540.

Hassanien M. A. and Abdel-Latif N. M. (2008) Polycyclic aromatic hydrocarbons in road dust over Greater Cairo, Egypt, *J. Hazardous Materials* 151, 247–254.

Iwasaki K., Ozaki N., Kojima K., and Kindaichi T. (2009) Estimation of river discharge loadings of PAHs in a suburban river in Hiroshima Prefecture, Japan, *J. Environment Technology*, 7(2), 109–120.

Kojima K., Kobayashi S., Kindaichi T. and Ozaki N. (2010) Modelling of wet deposition of atmospheric PAHs by the consecutive measurements in an urban area, Japan, *Water Science & Technology*, 62(8), 1922–1930.

Liu M., Cheng S. B., Ou D. N., Hou, L. J., Gao L., Wang, L. L., Xie, Y. S., Yang, Y. and Yu, S. Y. (2007) Characterization, identification of road dust PAHs in central Shanghai areas, China, *Atmospheric Environment*, 41, 8785–8795.

Ozaki N., Nitta K. and Fukushima T. (2006) Dispersion and dry and wet deposition of PAHs in an atmospheric environment, *Water Science & Technology*, 53(2), 215–224.

Ozaki N., Takeuchi S., Kojima K., Kindaichi T., Komatsu T. and Fukushima T. (2012) PAHs concentration and toxicity in organic solvent extracts of atmospheric particulate matter and sea sediments, *Water Science & Technology*, 66(5), 983–992.

Rogge, W.F., Hildemann, L.M., Mazurek, M.A., Cass, G.R. and Simoneit, B.R.T. (1993) Sources of fine organic aerosol. 3. Road dust, tire debris, and organometallic brake lining dust: roads as sources and sinks. *Environmental Science and Technology* 27(9), 1892–1904.

Thalheimer, W. and Cook, S. (2002). *How to calculate effect sizes from published research articles: A simplified methodology*. Retrieved October 22, 2014 from http://work-learning.com/effect_sizes.htm.

Thalheimer, W. and Cook, S. (2008). *How to calculate effect sizes from published research: A simplified spreadsheet*. Retrieved October 22, 2014 from <https://ja.scribd.com/doc/2902296/Effect-Sizes-Spreadsheet>.

Xue W. and Warshawsky D. (2005). Metabolic activation of polycyclic and heterocyclic aromatic hydrocarbons and DNA damage: A review, *Toxicology and Applied Pharmacology*, 206, 73–93.

Vinggaard A. M., Hnida C. and Larsen J. C. (2000). Environmental polycyclic aromatic hydrocarbons affect androgen receptor activation in vitro, *Toxicology*, 145, 159–169.

Yunker, M. B., MacDonald, R. W., Vingarzan, R., Mitchell, R., H., Goyette, D., and Sylvestre, S. (2002) PAHs in the Fraser River basin: a critical appraisal of PAH ratios as indicators of PAH source and composition, *Organic Geochemistry*, 33, 489–515.

Yunker, M. B. and MacDonald, R. W. (1995) Composition and origins of polycyclic aromatic hydrocarbons in the Mackenzie River and on the Beaufort Sea shelf, *Arctic*, 48, 118–129.

Zhang W., Zhang S., Wan C., Yue, D., Ye, Y. and Wang X. (2008) Source diagnostics of polycyclic aromatic hydrocarbons in urban road runoff, dust, rain and canopy throughfall, *Environmental Pollution*, 153, 594–601.